

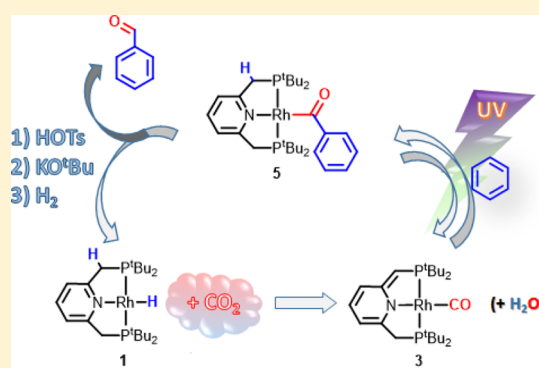
# Bottom-Up Construction of a CO<sub>2</sub>-Based Cycle for the Photocarbonylation of Benzene, Promoted by a Rhodium(I) Pincer Complex

Aviel Anaby,<sup>†</sup> Moran Feller,<sup>†</sup> Yehoshoa Ben-David,<sup>†</sup> Gregory Leitus,<sup>‡</sup> Yael Diskin-Posner,<sup>‡</sup> Linda J. W. Shimon,<sup>‡</sup> and David Milstein<sup>\*,†</sup>

Departments of <sup>†</sup>Organic Chemistry and <sup>‡</sup>Chemical Research Support, Weizmann Institute of Science, Rehovot 76100, Israel

**S** Supporting Information

**ABSTRACT:** The use of carbon dioxide for synthetic applications presents a major goal in modern homogeneous catalysis. Rhodium–hydride PNP pincer complex **1** is shown to add CO<sub>2</sub> in two disparate pathways: one is the expected insertion of CO<sub>2</sub> into the metal–hydride bond, and the other leads to reductive cleavage of CO<sub>2</sub>, involving metal–ligand cooperation. The resultant rhodium–carbonyl complex was found to be photoactive, enabling the activation of benzene and formation of a new benzoyl complex. Organometallic intermediate species were observed and characterized by NMR spectroscopy and X-ray crystallography. Based on the series of individual transformations, a sequence for the photocarbonylation of benzene using CO<sub>2</sub> as the feedstock was constructed and demonstrated for the production of benzaldehyde from benzene.



## INTRODUCTION

CO<sub>2</sub> presents an appealing one-carbon synthon for the chemical industry, and its direct incorporation into complex molecules is highly desirable.<sup>1–6</sup> It is thermodynamically challenging to reduce CO<sub>2</sub> in a clean and useful manner.<sup>2d,6c,7</sup> Reductive “splitting” or cleavage of CO<sub>2</sub> is possible, involving either oxygen transfer<sup>2b,8–15</sup> or disproportionation to carbonates<sup>8,16,17</sup> or, more commonly, to carbon monoxide and water in the reverse water–gas shift reaction (r-WGSR).<sup>1b,18–20</sup> An efficient and selective process for CO<sub>2</sub> splitting to CO and water is highly beneficial toward CO<sub>2</sub> utilization as a viable synthon.<sup>1b,c,3,4,6c,7,21a</sup> The use of hydrogen as the reducing agent is an atom-efficient means to convert CO<sub>2</sub> into useful compounds.<sup>21b–d</sup> For several decades, many organometallic complexes have been suggested as potential homogeneous catalysts for the reduction of CO<sub>2</sub> by hydrogen. Within this context, the insertion reaction of CO<sub>2</sub> into metal–hydride bonds has been the focus of many studies. While in some cases it has been implied that a nucleophilic attack of the hydride on the CO<sub>2</sub> carbon initiated the insertion,<sup>22</sup> it has been largely accepted to follow  $\pi$ -coordination of the CO<sub>2</sub> to the metal center, and subsequent  $\sigma$ -bond metathesis to afford a formate ligand.<sup>6c,18b,21a,b,23</sup> Consequently, homogeneous hydrogenation of CO<sub>2</sub> to formic acid (or salts thereof) has been achieved using metal complexes as catalysts.<sup>23d,24–31</sup> Moreover, since this process is reversible, formic acid has been proposed as a potential hydrogen chemical storage system.<sup>21c,26c,32–34</sup> Most outstanding are the highly efficient iridium-catalyzed hydrogenation of CO<sub>2</sub> reported by Nozaki et al.,<sup>26a,35</sup> and the

relatively benign iron-catalyzed CO<sub>2</sub> hydrogenation.<sup>26b,27</sup> Alternatively, products of CO<sub>2</sub> hydrogenation, including methanol<sup>14,21d,32a,36</sup> and formic acid, may be useful as reagents in further chemical transformations.<sup>6b,e,11,37</sup> Rather efficient rhodium catalysts for the hydrogenation of CO<sub>2</sub> have been reported by Leitner et al. and others,<sup>24,30</sup> achieving good turnover numbers (TON) under mild conditions. The insertion of CO<sub>2</sub> into the Rh–H bond of model Rh(I) and Rh(III) complexes is well studied.<sup>22b,d,24c,38</sup> It has been suggested that, while for Rh(I) complexes CO<sub>2</sub> insertion to afford a formate complex is facile, elimination of the formate product is rate limiting, whereas for Rh(III) complexes the actual insertion of CO<sub>2</sub> into the Rh–H bond is rate determining.<sup>39</sup> Chirik et al. demonstrated the facile insertion of CO<sub>2</sub> into the Co–H bond of a PNP (2,6-bis(di-*tert*-butylphosphinomethyl)pyridine) pincer complex, resulting in a stable formate complex.<sup>19</sup> The catalytic hydrosilylation of CO<sub>2</sub> was demonstrated by Chirik et al., albeit hampered by the eventual formation of the corresponding cobalt–carbonyl complex, likely as a result of CO<sub>2</sub> cleavage under the reaction conditions.<sup>19</sup>

In the past decade, our group has studied metal–ligand cooperation (MLC)<sup>40</sup> in activation of substrates such as alcohols,<sup>41</sup> amines,<sup>42</sup> nitriles,<sup>43</sup> boranes,<sup>44</sup> dihydrogen,<sup>45–47</sup> and dioxygen.<sup>48</sup> Relying on the potential of pyridine-based pincer complexes to undergo aromatization–dearomatization cycles, a novel mode of chemical bond activation was

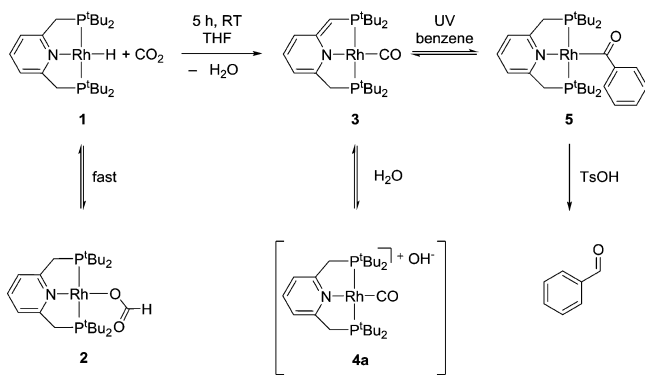
Received: May 18, 2016

Published: July 11, 2016

discovered, leading to efficient and benign catalytic transformation, most useful in hydrogenation, and dehydrogenation reactions.<sup>40b,c,49</sup> The interaction of pincer complexes with CO<sub>2</sub> was shown, in some cases, to entail the addition of CO<sub>2</sub> to the dearomatized ligand backbone, when the  $\pi$ -acidic carbon of CO<sub>2</sub> resides on the pincer ligand benzylic position.<sup>29a,50</sup> Recently our group has observed that, in the case of an iridium–hydride PNP complex, CO<sub>2</sub> is incorporated at the ligand benzylic position as a resting state, but is subsequently protonated via MLC and cleaved at the metal center to afford water and a CO ligand.<sup>51</sup>

Here we report on a pincer Rh(I)–H-promoted splitting of CO<sub>2</sub> by MLC, leading to a dearomatized Rh(I) carbonyl complex which, upon UV irradiation, C–H-activates benzene. Protonation of the resulting benzoyl complex leads to benzaldehyde (Scheme 1). Deprotonation and hydrogenation

### Scheme 1. CO<sub>2</sub> Cleavage and Photocarbonylation of Benzene



of the rhodium complex closes a novel MLC-promoted stoichiometric cycle, which can be repeated consecutively, for the formation of benzaldehyde from CO<sub>2</sub> and benzene.

## RESULTS AND DISCUSSION

Carbon dioxide reacts instantly at room temperature with the (PNP)RhH complex **1**.<sup>46</sup> Upon addition of 1 equiv, or more, of CO<sub>2</sub> gas to complex **1** in THF, the immediate product observed by NMR spectroscopy is the formate complex **2** (Scheme 1). Complex **2** exhibits a proton signal in the <sup>1</sup>H NMR spectrum at 8.6 ppm (dt, <sup>3</sup>J<sub>RhH</sub> = 2.8 Hz, <sup>4</sup>J<sub>PH</sub> = 1.4 Hz) which is consistent with a formyl proton. The symmetric <sup>1</sup>H NMR pattern of the ligand backbone, as well as the doublet signal in the <sup>31</sup>P{<sup>1</sup>H} NMR (60 ppm, <sup>1</sup>J<sub>RhP</sub> = 154 Hz) are indicative of an aromatized square planar Rh(I) complex.

X-ray crystallography of crystals of complex **2**, obtained by low temperature crystallization, indicated an  $\eta^1$ -OCHO structure (Figure 1), analogous to that of the cobalt–formate complex, reported by Chirik et al.<sup>19</sup> Van der Vlugt et al. recently observed a Rh(I)–formate complex as an intermediate in catalytic formic acid decomposition,<sup>34</sup> although the formate proton's <sup>1</sup>H NMR signal was not reported. Complex **2** is not stable, even at low temperatures, and cannot be separated from the reaction solution. When vacuum is applied to a solution containing complex **2**, CO<sub>2</sub> is extruded and complex **1** reforms; when complex **2** is kept in solution, the color slowly changes from orange to red, and monitoring by NMR spectroscopy confirms the formation of the dearomatized

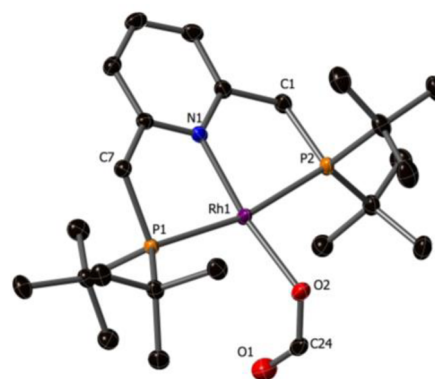


**Figure 1.** ORTEP representation of complex **2**, with thermal ellipsoids at 50% probability. Hydrogen atoms omitted for clarity. One of two discrete formate geometries in the asymmetric unit shown. Selected bond lengths [Å] and bond angles [°]: C24–O1, 1.214(4); C24–O2, 1.270(4); O2–Rh1, 2.075(2); Rh1–O2–C24, 128.0(2); O2–C24–O1, 130.0(3); N1–Rh1–O2, 169.02(6); P1–Rh1–P2, 167.62(2).

(PNP\*)RhCO complex **3**<sup>46</sup> (PNP\* = deprotonated PNP pincer ligand, Scheme 1), within 5 h at room temperature.

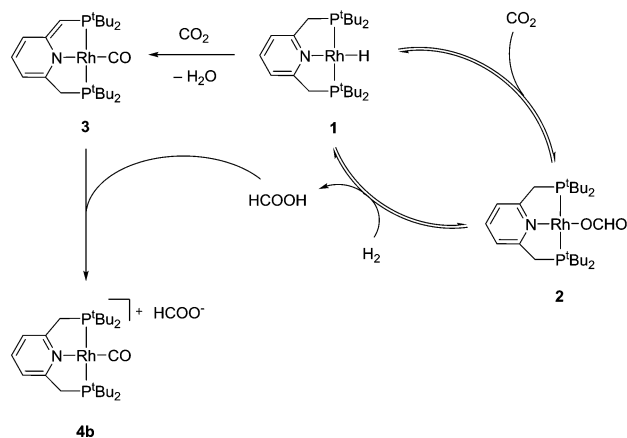
Conversion to the carbonyl complex **3** indicates apparent splitting of the CO<sub>2</sub> to CO and water. Water formation could not be unequivocally asserted, yet it is expected by stoichiometry, and observed in CO<sub>2</sub> activation by the analogous (PNP)IrH pincer complex.<sup>51</sup>

The reaction of complex **1** with CO<sub>2</sub> was monitored by variable temperature NMR spectroscopy, in acetone-*d*<sub>6</sub> (Figure S21). Rapid formation of complex **2** occurred even at 200 K. When raising the temperature to 250 K for 90 min, complex **3** was observed to form alongside the cationic rhodium–carbonyl complex, [(PNP)RhCO]X, which exhibits a doublet in the <sup>31</sup>P{<sup>1</sup>H} NMR at 79.8 ppm (<sup>1</sup>J<sub>RhP</sub> = 120.1 Hz). The cationic rhodium–carbonyl complex (with X = BF<sub>4</sub>, BARf, OC(O)CF<sub>3</sub>, Cl) was previously reported by our group.<sup>52</sup> Attempts to isolate and fully characterize this complex resulted in formation of complex **3**. It is plausible that the cationic complex is **4a** (Scheme 1), possessing a hydroxide counteranion. Upon solvation, or isolation, the basic counterion would deprotonate the benzylic proton of the ligand, yielding the dearomatized product, complex **3**, and water. Complex **4a** is observed independently when water is added to complex **3**, with a characteristic <sup>31</sup>P{<sup>1</sup>H} NMR signal at 79.4 ppm (d, <sup>1</sup>J<sub>RhP</sub> = 122 Hz). Complex **4a** was only observed as a product of CO<sub>2</sub> cleavage when the experiment was run in polar solvents at low temperatures. The possibility of a bicarbonate formation<sup>16,38f</sup> is less likely, since in that case the process is unlikely to be reversible, due to the bicarbonate anion mild basicity. The ratio between complexes **4a** and **3** in solution was found to be temperature dependent,<sup>53</sup> with complex **4a** being the major product in solution at lower temperatures (1.6:1 of **4a**/**3** at 220 K) and complex **3** becoming the major species at elevated temperatures (1:1.5 of **4a**/**3** at 273 K).

Catalytic hydrogenations of CO<sub>2</sub> by complex **1** were attempted. Following a similar protocol to that of Leitner et al.,<sup>24b,c</sup> a 1:5 triethylamine/THF solution of complex **1** (0.01 mM) was pressurized to 40 bar of H<sub>2</sub> and CO<sub>2</sub> (at 1:1 ratio) and stirred for 20 h at room temperature. A turnover number of 23 was observed toward the formation of the triethylammonium salt of formic acid. When the reaction was repeated without base,<sup>29b</sup> a TON of 7 was measured. Analysis of the

solutions after reaction by NMR spectroscopy revealed that, in both cases, complex **1** was consumed and the cationic rhodium–carbonyl complex **4b** ( $^{31}\text{P}\{^1\text{H}\}$  NMR signal at 79.5 ppm, d,  $^1J_{\text{RhP}} = 120$  Hz) was formed with a formate counteranion (Scheme 2). Thus, it appears that on the one

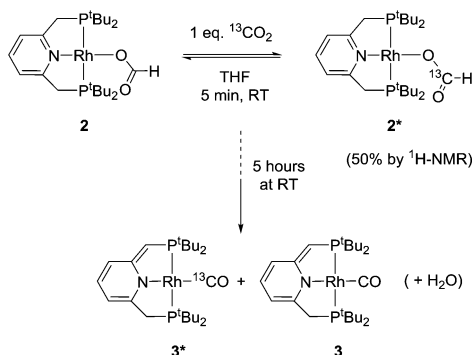
**Scheme 2. Reduction of  $\text{CO}_2$  by Complex 1**



hand, rhodium complex **1** readily undergoes insertion of  $\text{CO}_2$  into the metal–hydride bond, forming the formate complex **2** which may be hydrogenated back to complex **1**, eliminating formic acid; on the other hand,  $\text{CO}_2$  cleavage to form **3** eventually halts the reaction, stopping efficient hydrogenation of  $\text{CO}_2$  to formic acid (Scheme 2).

The insertion of  $\text{CO}_2$  into the Rh–H bond of complex **1** and rapid formation of complex **2** is, evidently, a reversible process. As aforementioned, complex **2** reverts to complex **1** under reduced pressure. A spin saturation transfer  $^1\text{H}$  NMR experiment confirmed the chemical exchange between the hydride of complex **1** and the formate proton of complex **2** in solution (Figure S20). Moreover,  $^{13}\text{C}$  labeled  $\text{CO}_2$  addition to nonlabeled complex **2** (formed *in situ* by addition of 1 equiv of  $\text{CO}_2$  gas to a THF solution of complex **1**) results in formation of the  $^{13}\text{C}$  labeled complex **2**, and eventually to the  $^{13}\text{C}$  labeled complex **3** (depicted as **2\***, and **3\***, respectively, Scheme 3).

**Scheme 3. Isotopic Labeling Experiment**



Notably, when 1 equiv of  $\text{CO}_2$  is added to a water/THF (2:3) solution of complex **1**, the solution color turns within seconds from brown to yellow, and NMR spectroscopy indicates the exclusive formation of the cationic rhodium–carbonyl complex **4a** ( $^{31}\text{P}\{^1\text{H}\}$  NMR signal at 79.5 ppm, d,  $^1J_{\text{RhP}} = 120$  Hz), which is the product of protonation of

complex **3** by water. Complex **2** is not detected at all in the aqueous solution, and may either have been very rapidly consumed, or not have formed altogether. The accelerating effect of water on processes involving metal ligand cooperation is well documented.<sup>51,54</sup>

The insertion pathway, leading to the formation of complex **2**, matches that of the analogous PNP pincer complex of cobalt, observed by Chirik et al.<sup>19</sup> The second pathway, resulting in the splitting of  $\text{CO}_2$ , has been observed in our group as the prevailing outcome of  $\text{CO}_2$  reaction with the analogous iridium PNP pincer complex.<sup>51</sup> The duality of rhodium–hydride complex **1** in reaction with  $\text{CO}_2$  demonstrates elegantly the trend in reactivity when descending down the ninth column of the periodic table. Although it cannot be unequivocally asserted at this point, we believe the mechanism leading to the formation of complex **3** from complex **1** and  $\text{CO}_2$  is disparate from the reversible insertion pathway leading to the formate complex **2**.<sup>6b,21b,55</sup> Complex **2** is the product of facile insertion of  $\text{CO}_2$  into the metal–hydride bond.<sup>19,24a,c,38a,d,56</sup> The process leading to  $\text{CO}_2$  cleavage is slower and apparently, in our case, irreversible. As of yet, we could not find compelling evidence to support a mechanistic pathway for the observed  $\text{CO}_2$  cleavage (formally, a r-WGSR) by complex **1**. It likely follows a similar pathway to that observed for the analogous iridium complex.<sup>51</sup> This may entail an  $\eta^1\text{-CO}_2$  coordination, forming an elusive and unstable carboxylate intermediate,<sup>1a,8,15,21,55,57</sup> which may then be protonated and dehydroxylated,<sup>58</sup> through metal–ligand cooperation, to yield a carbonyl ligand (complex **3**) and water.<sup>51</sup> Alternatively, other mechanistic pathways may be conceived, such as disproportionation,<sup>8,16,38f</sup> decarbonylation,<sup>19,38b</sup> or dehydration of the formate.<sup>32a,58</sup> Formation of complex **3** and water may serve as a thermodynamic sink that drives the system toward  $\text{CO}_2$  cleavage rather than formate formation.

While reductive cleavage of  $\text{CO}_2$  with no net change in the oxidation state of the rhodium metal is remarkable in itself, the resultant dearomatized monocarbonyl product complex of this stoichiometric reaction is known to be quite unreactive.<sup>46,52</sup> It was thus gratifying to discover that, upon irradiating a benzene solution of the dearomatized monocarbonyl complex **3** under UV(B) (Luzchem LZC-UVB lamps with peak intensity at 320 nm), gradual formation of the benzoyl complex **5** is observed. Conversion to complex **5** reaches 50–80% (by NMR spectroscopy) in solution, after 72 h irradiation (Figure 2). Intermediates of the carbonylation reaction could not be observed. The only other products observable by NMR spectroscopy are the previously reported (PNP)RhPh complex **6**<sup>46,59</sup> (15–45% by integration after 72 h under UV(B)), and residual carbonyl complex **3**.

The spectral assignment of the benzoyl complex was confirmed when complex **5** was synthesized independently from the dearomatized dinitrogen complex **7**<sup>59</sup> under reduced pressure (facilitating ligand exchange) with 1 equiv of benzaldehyde in benzene (Scheme 4). Complex **5** thus obtained was also crystallized and its structure elucidated by X-ray crystallography (Figure 3).

The variability in the relative amounts of the benzoyl complex **5** and the phenyl complex **6** arises from variable reaction conditions, such as type of vessel, amount and concentration of solution and ambient temperatures. It became evident that CO loss during irradiation leads to increased formation of complex **6**, at the expense of complex **5**.



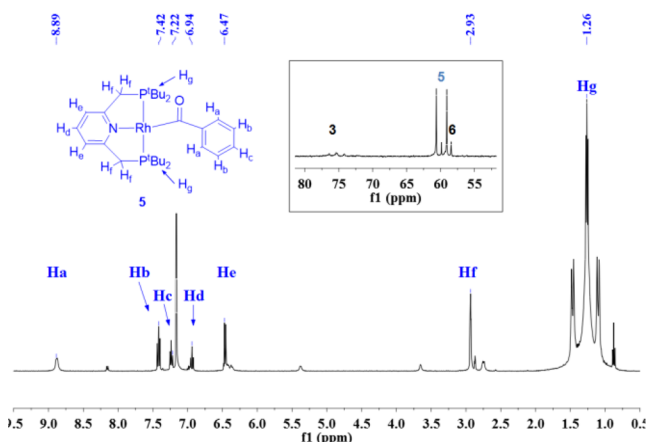


**Figure 2.**  $^1\text{H}$  NMR spectrum (benzene- $d_6$ , 400 MHz) of the resulting mixture after irradiation of complex **3** in benzene for 72 h under UV(B). Signal assignments for complex **5** are in blue. Inset:  $^{31}\text{P}\{^1\text{H}\}$  NMR spectrum (benzene- $d_6$ , 122 MHz) of the corresponding mixture.

#### Scheme 4. Independent Synthesis of Complex 5

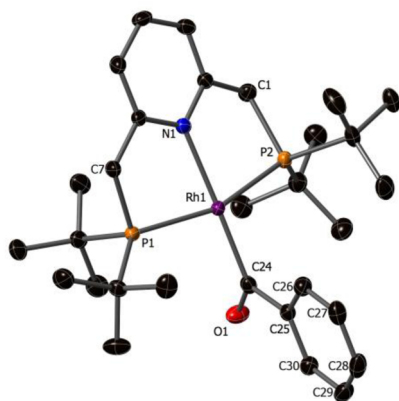
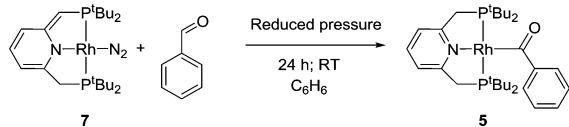


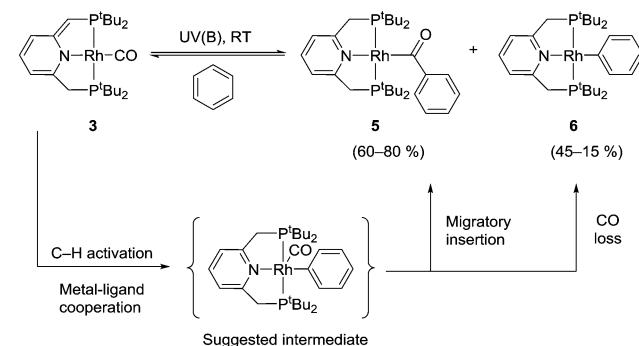
**Figure 3.** ORTEP representation of complex **5**, with thermal ellipsoids at 50% probability. Hydrogen atoms omitted for clarity. One of two identical molecules in the asymmetric unit shown. Selected bond lengths [Å] and bond angles [ $^\circ$ ]: C24–O1, 1.235(2); C24–C25, 1.534(3); C24–Rh1, 1.993(2); Rh1–C24–O1, 124.7(2); Rh1–C24–C25, 120.9(1); O1–C24–C25, 114.4(2).

Indeed, when the irradiation of a benzene solution of complex **3** is carried out with minimal headspace over the solution, that is, the solution occupies nearly the whole vessel volume, complex **5** is consistently formed in 65% yield (by NMR, after 72 h irradiation). When a benzene solution of complex **3** is irradiated under UV(B) in a vessel with a large headspace volume, rhodium–phenyl complex **6** is formed almost exclusively within a 72 h irradiation period.

Although a radical mechanism cannot be excluded for the photocarbonylation reaction,<sup>60,61</sup> and while early studies had suggested the possibility of a dissociative mechanism (ligand or CO extrusion) to lead to C–H activation;<sup>62</sup> exhaustive mechanistic research, conducted by Goldman,<sup>61</sup> and Field<sup>63</sup> on rhodium-catalyzed photocarbonylation of benzene<sup>64–66</sup>

suggests that it may proceed by an associative mechanism, whereby UV irradiation excites the rhodium carbonyl complex **3**, enabling C–H activation of benzene. In the case of the PNP pincer complex **3**, C–H activation by MLC leads to re-aromatization of the pincer ligand, which may serve as a driving force for this reaction. The postulated pentacoordinate intermediate (Scheme 5) would undergo migratory insertion,<sup>67</sup>

#### Scheme 5. Photocarbonylation Reaction of Complex 3 in Benzene



resulting in the square planar complex **5**. CO loss, evident by the formation of complex **6**, may also be expected to occur from the suggested pentacoordinate rhodium species under the reaction conditions.<sup>61,65</sup> The main mechanistic difference in the photocarbonylation of benzene by complex **3**, versus that of the Vaska-type rhodium complexes,<sup>61,63,64a,66</sup> is that benzene activation by the Rh(I) takes place by metal–ligand cooperation, and hence the product is a Rh(I) benzoyl complex (rather than Rh(III)), with no overall change in the metal oxidation state.

A competition experiment was conducted in parallel, with two separate J. Young NMR tubes charged with the same amount and concentrations of complex **3**: the one in  $\text{C}_6\text{H}_6$ , and the second in  $\text{C}_6\text{D}_6$ . Both solutions were irradiated for 72 h simultaneously under UV(B). Whereas only partial conversion was achieved in the deuterated solvent, with ratios of 13:5:3 of complexes **3**/**5**/**6**, the sample in regular benzene showed full conversion, with 4:1 ratio of complexes **5**/**6**. This result indicates C–H activation to be the rate-limiting step in the photocarbonylation reaction. Moreover, the splitting of the corresponding signals in the  $^{31}\text{P}\{^1\text{H}\}$  NMR spectrum (Figure S37) indicate deuterium incorporation in the ligand backbone of complex **3** after irradiation in benzene- $d_6$ , which supports the suggested reversible formation of a phenyl-carbonyl rhodium intermediate. Complex **5** is also observed upon addition of CO gas to a solution of complex **6** (Figure S40). Complex **3** is also formed in this case, demonstrating both the ease of migratory insertion, and the reversibility of the carbonylation reaction.<sup>68</sup>

Since the source of the carbonyl group is  $\text{CO}_2$  (Scheme 1), this simple photocarbonylation method holds promise as an alternative to the reported processes based on carbon monoxide.<sup>61,65,66,69</sup> Nevertheless, in order for this to present a viable catalytic process, it is essential to promote product release from the benzoyl complex **5**. The addition of CO gas to the photoreaction product solution, containing complexes **5** and **6**, did result in formation of free benzaldehyde and the dearomatized carbonyl complex **3**. Moreover, irradiation of a benzene solution of complex **3** under an atmosphere of CO gas allows for catalytic formation of benzaldehyde (Figure S41).

The observed photocarbonylation of benzene with a pincer rhodium(I) complex is quite unique, and relies on MLC to trap the C–H activated species (Scheme 5). Nevertheless, rhodium-catalyzed photocarbonylation of benzene under CO atmosphere is known and well studied.<sup>61–66</sup>

Pressurizing complex 5 under N<sub>2</sub>, H<sub>2</sub>, or CO<sub>2</sub> gas (or a combination thereof) did not result in significant release of benzaldehyde. Addition of methanol, ethanol, phenol, or trifluoroethanol was also attempted for the release of an acylated product from complex 5, but with no success. Finally, it was found that strong organic protic acids promote the release of free benzaldehyde from complex 5, in up to 50% yield. While trifluoromethanesulfonic acid and diphenylacetic acid both enabled the release of benzaldehyde (Figures S50 and S51), *p*-toluenesulfonic acid (TsOH) was found to be the most suitable for this purpose, providing a more “well-behaved” system that was convenient to monitor and study. Thus, upon addition of 1 equiv of TsOH to a benzene solution of complex 5, initially only a slight color change is observed, from dark brown to a slightly lighter brown solution. NMR spectroscopy reveals that one major complex is formed, with a similar <sup>1</sup>H NMR pattern to that of complex 5, and a <sup>31</sup>P{<sup>1</sup>H} NMR signal at 62 ppm (d, <sup>1</sup>J<sub>RhP</sub> = 117 Hz). In addition, a new hydride signal is observed in the <sup>1</sup>H NMR spectrum (dt, <sup>1</sup>J<sub>RhH</sub> = 31 Hz, <sup>2</sup>J<sub>PH</sub> = 11 Hz). These spectral features indicate a rhodium(III) hydrido-benzoyl-tosylate complex (complex 8, Scheme 6). The solubility of this complex in nonpolar solvents (even at low temperatures), as well as the hydride chemical shift and the Rh–P coupling constant all indicate a charge neutral octahedral rhodium(III) complex, with the TsO<sup>−</sup> ligand coordinated (possibly weakly).<sup>42c,52</sup> Complex 8 was observed for several

hours in solution at low temperature; however, it could not be isolated. Within an hour at room temperature, the solution color changes to bright orange and two new major complexes are observed by NMR spectroscopy, with disappearance of complex 8.

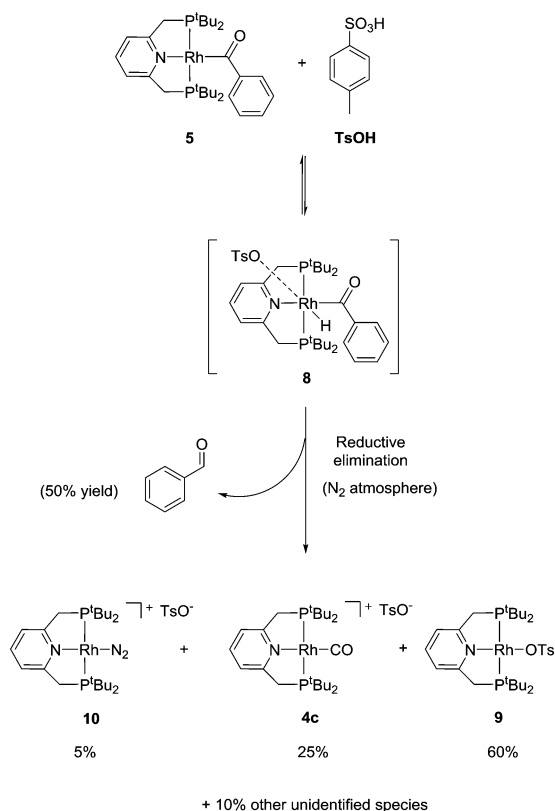
Most importantly, a clear signal of free benzaldehyde is observed in the <sup>1</sup>H NMR spectrum. One new complex can be assigned to the cationic rhodium carbonyl complex (4c, Scheme 6), with a TsO<sup>−</sup> counterion. This may be a result of decarbonylation of the benzoyl complexes (either 5 or 8), protonated by the added TsOH. The major product complex, appearing as a doublet in the <sup>31</sup>P{<sup>1</sup>H} NMR spectrum at 60 ppm (<sup>1</sup>J<sub>RhP</sub> = 147 Hz) with no corresponding hydride, was assigned as (PNP)RhOTs complex 9 (Scheme 6). A third species appears as a doublet in the <sup>31</sup>P{<sup>1</sup>H} NMR spectrum at 72 ppm (<sup>1</sup>J<sub>RhP</sub> = 125 Hz), which is likely the cationic Rh–N<sub>2</sub> complex 10 (with a TsO<sup>−</sup> counterion, Scheme 6), that may form under the nitrogen atmosphere. Other minor species with similar spectral features to complex 9 appear after several hours; however, those could not be identified nor isolated. Thus, oxidative addition of TsOH to the rhodium(I) benzoyl complex 5 results in a rhodium(III) hydrido-benzoyl complex (8) which readily reductively eliminates benzaldehyde and forms the rhodium(I) complexes 9 and 10. Complex 9 was also crystallized out of the product mixture and characterized by X-ray spectroscopy (Figure S54). Both complexes 9 and 10 could be obtained as a mixture when adding 1 equiv of TsOH to a solution of complex 7, in line with their assignments. The assignment of complex 4c was corroborated by its independent synthesis from complex 3 and TsOH. The yield of benzaldehyde from this process was measured with an internal standard to be 50% (Figure S53). Isolated yield (by vacuum distillation) is lower, due to the small scale. Yield loss may be explained by the competing decarbonylation reaction that occurs thermally under these conditions.<sup>61,64,70</sup> Finally, after removing the volatiles (including the benzaldehyde product), it was possible to re-form complex 1 (alongside complex 3): Addition of 1 equiv of potassium *tert*-butoxide base to the aforementioned complex mixture (9, 10, 4c, and the unknowns), followed by filtration in pentane and hydrogenation under 5.5 bar hydrogen gas, results in a binary mixture of complexes 1 and 3, that is again viable for the reductive cleavage of CO<sub>2</sub>, and subsequent photocarbonylation of benzene (Figures S58 and S59).

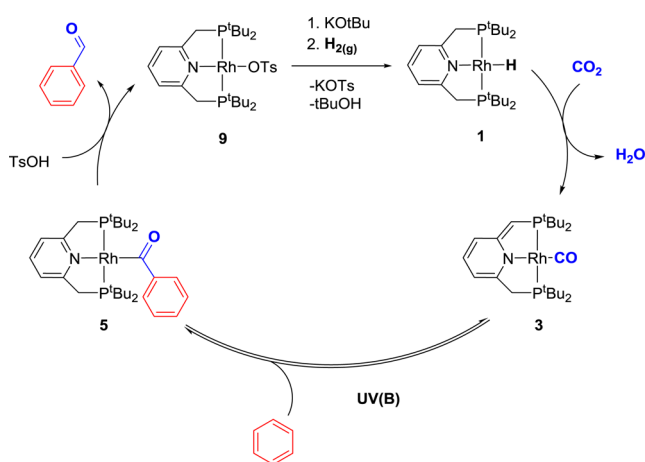
Although a full catalytic cycle for the photocarbonylation of benzene with CO<sub>2</sub> based on complex 1 is not achieved, it is possible to construct a cycle, in a bottom-up approach, by sequentially combining the individual stoichiometric steps described above. This has been achieved, experimentally, in milligram scale. The overall process is summarized schematically in Scheme 7, demonstrating the current capabilities of the CO<sub>2</sub> based photocarbonylation of benzene with the rhodium(I) PNP pincer complexes.<sup>71</sup> This process has been conducted in our laboratory, with an overall yield of 30% benzaldehyde isolated, relative to starting complex 1, in two consecutive cycles (Figures S55–S60).

## SUMMARY

Conceptually, a full stepwise cycle for the carbonylation of benzene using CO<sub>2</sub> was achieved. This is not a catalytic system, since the individual steps in the carbonylation cycle require variation of the conditions. Nevertheless, it does illustrate the possibility of combining MLC-based CO<sub>2</sub> splitting with further

### Scheme 6. Protonation of Complex 5 and Elimination of Benzaldehyde



Scheme 7. Stepwise Cycle for Carbonylation of Benzene with CO<sub>2</sub>

reactivity of the resulting metal carbonyl to yield benzaldehyde. The prospect of a PNP rhodium pincer catalytic system for arene carbonylation with CO<sub>2</sub>, potentially replacing the carbon monoxide-based process, as well as possibly further derivatization of the produced aldehyde, leading to thermodynamically viable processes,<sup>71</sup> is a highly attractive goal. Tuning of the physical and chemical conditions of this system is beyond the scope of this article, and we are currently striving to transform this from a stepwise reaction series, into a catalytic cycle.

## EXPERIMENTAL SECTION

**General.** Rhodium complexes **1**, **3**, **6**, and **7** were synthesized according to previously reported methods.<sup>46,59</sup> All organic reagents were purchased from commercial sources without further purification. All solvents used were dried and distilled according to known procedures to ensure purity and absence of water. CO<sub>2</sub> gas, H<sub>2</sub> gas, and CO gas were all purchased from commercial sources in high-pressure cylinders and used without further purification using Schlenk techniques. <sup>13</sup>C labeled CO, and CO<sub>2</sub> gases were purchased from commercial sources in lecture bottles and used without further purification using Schlenk techniques. All reactions were carried out inside a nitrogen atmosphere glovebox or using Schlenk techniques to ensure oxygen and external water free environments. Photoreactions were carried out in a Luzchem LZC-ORG chamber, equipped with 10 LZC-UVB side lamps, with peak intensity at 320 nm. <sup>1</sup>H, <sup>13</sup>C, and <sup>31</sup>P NMR spectra were recorded using Bruker AMX-300, AMX-400, or AMX-500 NMR spectrometers. <sup>1</sup>H and <sup>13</sup>C chemical shifts are reported in ppm downfield from tetramethylsilane and referenced to residual protonated solvent shifts.<sup>72</sup> <sup>31</sup>P NMR chemical shifts are referenced to an external 85% solution of phosphoric acid in D<sub>2</sub>O. All spectra were recorded at 298 K unless otherwise indicated. Temperature calibration of the spectrometer was performed using CH<sub>3</sub>OH/CD<sub>3</sub>OD. Abbreviations used in the NMR spectral assignments: b, broad; s, singlet; d, doublet; dd, doublet of doublets; t, triplet; q, quartet; m, multiplet; v, virtual.

**Reaction of Complex 1 with CO<sub>2</sub>: In Situ Formation of (PNP)Rh(OCHO) (2).** In a dry nitrogen glovebox, complex **1** (10.0 mg, 0.02 mmol) was dissolved in toluene-*d*<sub>8</sub> (0.5 mL) in an NMR tube and sealed with a septum cap. The tube was taken out of the glovebox, and CO<sub>2</sub> (488 μL, at 1 bar) was injected through the septum cap using a gastight microsyringe. Upon shaking of the tube, the dark brown solution turned slightly orange within seconds. Complex **2** could not be isolated, as it gradually converted thermally in solution to complex **3**, or, upon evaporation of the solution under vacuum, it converted to complex **1**. NMR spectroscopic data were taken at 278 K: <sup>1</sup>H NMR (400 MHz, toluene-*d*<sub>8</sub>, δ): 8.58 (dt, <sup>3</sup>J<sub>RhH</sub> = 2.8 Hz, <sup>4</sup>J<sub>PH</sub> = 1.4 Hz, 1H, RhOCHO), 6.89 (t, <sup>3</sup>J<sub>HH</sub> = 7.7 Hz, 1H, Py-H4), 6.25 (d, <sup>3</sup>J<sub>HH</sub> = 7.6

Hz, 2H, Py-H3,5), 2.52 (vt, <sup>1</sup>J<sub>PH</sub> = 3.4 Hz, 4H, CH<sub>2</sub>P), 1.40–1.34 (bvt, <sup>1</sup>J<sub>PH</sub> = 6.4, 6.5 Hz, 36H, PC(CH<sub>3</sub>)<sub>3</sub>) ppm; <sup>13</sup>C{<sup>1</sup>H} NMR (101 MHz, toluene-*d*<sub>8</sub>, verified by HSQC, δ): 168.11 (b, RhOCHO), 164.56 (dvt, <sup>1</sup>J<sub>PC</sub> = 6.4 Hz, <sup>2</sup>J<sub>RhC</sub> = 1.2 Hz, Py-C2,6), 129.76 (s, Py-C4) 119.57 (dvt, <sup>1</sup>J<sub>PC</sub> = 5.1 Hz, <sup>3</sup>J<sub>RhC</sub> = 1.0 Hz, Py-C3,5), 35.69 (dvt, <sup>1</sup>J<sub>PC</sub> = 5.5 Hz, <sup>2</sup>J<sub>RhC</sub> = 0.9 Hz, CH<sub>2</sub>P), 34.47 (dvt, <sup>1</sup>J<sub>PC</sub> = 5.6 Hz, <sup>2</sup>J<sub>RhC</sub> = 1.4 Hz, PC(CH<sub>3</sub>)<sub>3</sub>), 29.32 (vt, <sup>1</sup>J<sub>PC</sub> = 3.7 Hz, PC(CH<sub>3</sub>)<sub>3</sub>) ppm; <sup>31</sup>P{<sup>1</sup>H} NMR (162 MHz, toluene-*d*<sub>8</sub>, δ): 60.0 (d, <sup>1</sup>J<sub>RhP</sub> = 154.2 Hz) ppm.

Red crystals of complex **2**, suitable for X-ray crystallography, were obtained by 5 s bubbling of CO<sub>2</sub> into a toluene solution of complex **1** (10 mg of complex in 0.5 mL of toluene), followed by addition of pentane (2 mL to the product toluene solution of complex **2**) and keeping at –30 °C for 24 h. Crystallographic data are given in Table S1 and the CIF file.

**Prolonged Reaction of Complex 1 with CO<sub>2</sub> in THF: Formation of (PNP\*)RhCO (3).** In a dry nitrogen glovebox, complex **1** (10.0 mg, 0.02 mmol) was dissolved in THF (0.5 mL) in an NMR tube and sealed with a septum cap. The tube was taken out of the glovebox and CO<sub>2</sub> (488 μL, at 1 bar) was injected through the septum cap using a gastight micro syringe. Upon shaking of the tube, the dark brown solution turned slightly orange within seconds (formation of complex **2**). The tube was then shaken for 5 h at ambient temperature, during which the solution color gradually turned to red. NMR spectroscopy confirmed quantitative conversion to complex **3**.

Complex **3** was characterized in a previous publication.<sup>46</sup> The UV–vis absorption spectrum and X-ray crystal structure are shown in Figures S33 and S34, respectively. Major UV–vis absorption bands (in pentane): 212, 290, 310, and 385 nm. Orange crystals suitable for X-ray diffraction were grown by slow evaporation of a heptane solution of complex **3**, under a dry nitrogen atmosphere, at room temperature. Crystallographic data are given in Table S1 and the CIF file.

**Reaction of Complex 1 with CO<sub>2</sub> in Water/THF Solution: In Situ Formation of [(PNP)RhCO]OH (4a).** In a dry nitrogen glovebox, complex **1** (7.5 mg, 0.015 mmol) was dissolved in THF (0.4 mL) in an NMR tube sealed with a septum cap. The tube was taken out of the glovebox and H<sub>2</sub>O (0.1 mL, deionized and degassed) was added. No significant changes to the spectral features of complex **1** were observed by NMR. CO<sub>2</sub> (336 μL, 1 equiv) was then injected by a gastight syringe to the NMR tube, at room temperature, and the tube was shaken vigorously for 5 min, then an NMR spectrum was recorded, showing full conversion to the cationic carbonyl complex **4a**. Partial <sup>1</sup>H NMR assignments (300 MHz, THF/water, δ): 8.02 (t, <sup>3</sup>J<sub>HH</sub> = 7.9 Hz, 1H, Py-H4), 7.71 (d, <sup>3</sup>J<sub>HH</sub> = 7.9 Hz, 2H, Py-H3,5), 1.40–1.38 (bvt, <sup>1</sup>J<sub>PH</sub> = 7.2, 7.3 Hz, 36H, PC(CH<sub>3</sub>)<sub>3</sub>) ppm; <sup>31</sup>P{<sup>1</sup>H} NMR (121 MHz, THF/water, δ): 79.5 (d, <sup>1</sup>J<sub>RhP</sub> = 120.3 Hz) ppm. Upon long evaporation of this solution under high vacuum and dissolution in dry THF, the color became red again, and a broad signal in the <sup>31</sup>P{<sup>1</sup>H} NMR (121 MHz, THF) at 72–76 ppm appeared, befitting complex **3**. Residual water is observed in the proton spectrum, accounting for the broad signals.

**Reaction of Complex 3 in Water/THF Solution: In Situ Formation of [(PNP)RhCO]OH (4a).** In a dry nitrogen glovebox, complex **3** (8 mg, 0.015 mmol) was dissolved in THF (0.4 mL) in an NMR tube sealed with a septum cap. The tube was taken out of the glovebox, H<sub>2</sub>O (0.2 mL, deionized and degassed) was added and the tube was shaken for 5 min. An immediate color change from red to yellow-orange was observed. An NMR spectrum was recorded, showing full conversion to the cationic carbonyl complex **4a**. Partial <sup>1</sup>H NMR assignments (300 MHz, THF/water, δ): 8.00 (b, 1H, Py-H4), 7.71 (b, 2H, Py-H3,5), 1.40–1.38 (bvt, <sup>1</sup>J<sub>PH</sub> = 7.1, 7.3 Hz, 36H, PC(CH<sub>3</sub>)<sub>3</sub>) ppm; <sup>31</sup>P{<sup>1</sup>H} NMR (121 MHz, THF/water, δ): 79.4 (bd, <sup>1</sup>J<sub>RhP</sub> = 122 Hz) ppm. These spectral features resemble that of previously reported [(PNP)RhCO]X (X = BF<sub>4</sub>, Bar<sup>f</sup>, OC(O)CF<sub>3</sub>, Cl).<sup>52</sup>

**Attempted Catalytic Hydrogenation of CO<sub>2</sub> to Formate Salt with NEt<sub>3</sub>.** *Caution!* H<sub>2</sub> gas is highly explosive, and appropriate safety measures should be taken when attempting these procedures. In a dry nitrogen glovebox, complex **1** (17 mg, 0.034 mmol) was charged into a Teflon-lined Parr autoclave, and dissolved in 3 mL of THF/NEt<sub>3</sub> (5:1) solution. The autoclave was taken out of the box and pressurized first



with 20 bar of H<sub>2</sub> gas, followed by an additional 20 bar CO<sub>2</sub> gas. After dissolution of the gases at room temperature, the pressure gauge registered a total of 36 bar. The solution was stirred at room temperature for 20 h. The vessel was then cooled to 0 °C and vented in a fume hood. The solution was concentrated under vacuum. Mesitylene (0.027 mmol) was added as standard, and NMR spectra were recorded in CDCl<sub>3</sub>. <sup>1</sup>H NMR (300 MHz) showed formation of 0.8 mmol formic acid–triethylamine adduct (TON = 23). <sup>31</sup>P{<sup>1</sup>H} NMR (121 MHz) showed a signal at 78.6 (d, <sup>1</sup>J<sub>RhP</sub> = 121 Hz) ppm, corresponding to complex **4b** (vide infra).

**Reaction of Complex 1 under High-Pressure CO<sub>2</sub> and H<sub>2</sub>: Formation of [(PNP)RhCO]CHO (4b).** *Caution! H<sub>2</sub> gas is highly explosive, and appropriate safety measures should be taken when attempting these procedures.* In a dry nitrogen glovebox, complex **1** (3.5 mg, 7 × 10<sup>-3</sup> mmol) was charged into a Teflon lined Parr autoclave, and dissolved in 3 mL of THF. The autoclave was taken out of the box and pressurized first with 30 bar of H<sub>2</sub> gas, followed by an additional 20 bar CO<sub>2</sub> gas. After dissolution of the gases, at room temperature, the pressure gauge registered a total of 42 bar. The solution was stirred at room temperature for 18 h. The vessel was then cooled to 0 °C and vented in a fume hood. A sample (0.5 mL) was taken of the product solution and a <sup>1</sup>H NMR spectrum was recorded, showing formation of complex **4b** and a signal befitting a formate moiety. An 8:1 ratio of the formate signal (8.1 ppm) versus the product complex signal (complex **4b**, signal at 7.97 ppm, t, Py-H4) was observed. The solution was evaporated under high vacuum and the residue dissolved in acetone-*d*<sub>6</sub> for NMR spectroscopy. Residual formic acid, and deuterium exchange affect the spectral features. Nevertheless, it is in line with previously reported cationic [(PNP)RhCO]<sup>+</sup> fragments.<sup>52</sup> <sup>1</sup>H NMR (400 MHz, acetone-*d*<sub>6</sub>, δ): 8.59 (b, 1H (overlapping with excess residual formic acid), HCOO), 8.04 (t, <sup>3</sup>J<sub>HH</sub> = 7.8 Hz, 1H, Py-H4), 7.74 (<sup>3</sup>J<sub>HH</sub> = 7.8 Hz, 2H, Py-H3,5), 4.18 (bm, 4H (2.8H by integration due to deuterium exchange), CH<sub>2</sub>P), 1.46 (m, 36H, PC(CH<sub>3</sub>)<sub>3</sub>) ppm; <sup>13</sup>C{<sup>1</sup>H} NMR (partial assignment, from HSQC, 400 MHz, acetone-*d*<sub>6</sub>, δ): 165.6 (HCOO), 138.0 (Py-C4), 122.4 (Py-C3,5), 36.4 (CH<sub>2</sub>P), 29.5 (PC(CH<sub>3</sub>)<sub>3</sub>) ppm; <sup>31</sup>P{<sup>1</sup>H} NMR (162 MHz, acetone-*d*<sub>6</sub>, δ): 79.48 (d, <sup>1</sup>J<sub>RhP</sub> = 120.6 Hz (fine deuterium coupling due to deuterium exchange on the ligand backbone, features a doublet of multiplet with J<sub>DP</sub> = 17 Hz).

**Photocarbonylation of Benzene by Complex 3: In Situ Formation of (PNP)RhCOPh (5).** In a dry nitrogen glovebox, complex **3** (10 mg, 0.019 mmol) was dissolved in benzene (0.5 mL). The tube was irradiated under UV(B), at ambient temperature, for 72 h. With irradiation, the solution color gradually turned from bright red to brown. The reaction was monitored by <sup>1</sup>H and <sup>31</sup>P NMR, showing formation of complexes 3/6/5 in 1:3:16 ratios, respectively. In-situ spectroscopic indication of complex **5**: <sup>1</sup>H NMR (300 MHz, benzene, δ): 8.86 (bd, <sup>3</sup>J<sub>HH</sub> = 6.3 Hz, Benzoyl-H2,6), 2.93 (b, CH<sub>2</sub>P), 1.25 (bm, PC(CH<sub>3</sub>)<sub>3</sub>) ppm; <sup>31</sup>P{<sup>1</sup>H} NMR (121.5 MHz, benzene, δ): 59.90 (d, <sup>1</sup>J<sub>RhP</sub> = 187.4 Hz) ppm. The formation of benzoyl complex **5** was also confirmed in situ by <sup>13</sup>C NMR, when starting from the <sup>13</sup>C labeled carbonyl complex **3** in the same experimental procedure: <sup>13</sup>C{<sup>1</sup>H} NMR (75 MHz, benzene, δ): 264.7 (dt, <sup>1</sup>J<sub>RhC</sub> = 34.5 Hz, <sup>2</sup>J<sub>PC</sub> = 8.6 Hz, RhCOPh) ppm. Full characterization of complex **5** (in mixture with complexes **3** and **6**) was possible after evaporation of the reaction solvent and dissolution in deuterated benzene. Full spectral assignment of complex **5** (ca. 75% in the mixture): <sup>1</sup>H NMR (400 MHz, benzene-*d*<sub>6</sub>, δ): 8.89 (bd, <sup>3</sup>J<sub>HH</sub> = 6.3 Hz, 1H Benzoyl-H2,6), 7.42 (m, 2H, Benzoyl-H3,5), 7.22 (m, 1H, Benzoyl-H4), 6.94 (t, <sup>3</sup>J<sub>HH</sub> = 7.6 Hz, 1H, Py-H4), 6.47 (d, <sup>3</sup>J<sub>HH</sub> = 7.6 Hz, 2H, Py-H3,5) 2.93 (vt, J<sub>PH</sub> = 2.9 Hz, 4H, CH<sub>2</sub>P), 1.26 (dd (looks like t), J<sub>PH</sub> = 6.1, 6.2 Hz, 36H, PC(CH<sub>3</sub>)<sub>3</sub>) ppm; <sup>13</sup>C{<sup>1</sup>H} NMR (100 MHz, benzene-*d*<sub>6</sub>, verified by HSQC and HMBC, δ): 264.7 (dt, <sup>1</sup>J<sub>RhC</sub> = 34.5 Hz, <sup>2</sup>J<sub>PC</sub> = 8.6 Hz, RhCOPh), 132.7 (Benzoyl-C2,6), 127.1 (Benzoyl-C3,5), 119.3 (Benzoyl-C4), 37.8 (vt, J<sub>PC</sub> = 5.0 Hz, CH<sub>2</sub>P), 35.5 (bm, PC(CH<sub>3</sub>)<sub>3</sub>), 30.0 (b, PC(CH<sub>3</sub>)<sub>3</sub>) ppm; <sup>31</sup>P{<sup>1</sup>H} NMR (121.5 MHz, benzene-*d*<sub>6</sub>, δ): 59.90 (d, <sup>1</sup>J<sub>RhP</sub> = 187.4 Hz) ppm.

**Independent Synthesis of (PNP)RhCOPh (5).** In a dry nitrogen glovebox, complex **7** (20 mg, 0.038 mmol) and benzaldehyde (4.8 mg, 1.2 equiv) were dissolved in benzene (1.5 mL) inside a Schlenk tube.

The solution was frozen in liquid nitrogen and vacuum was applied for 30 s, to reduce the partial pressure of nitrogen gas. The solution was stirred for 12 h under reduced pressure, at ambient temperature. The red solution turned greenish-brown, with >95% formation (by <sup>1</sup>H NMR) of complex **5**, with identical spectroscopic assignment to that formed by photocarbonylation (above). Crystals suitable for X-ray diffraction were grown by the dissolution of complex **5** in minimum pentane containing benzaldehyde (1 equiv excess), keeping at -30 °C for a week. Crystallographic data are given in Table S1 and the CIF file.

**Reaction of Complex 5 with TsOH: In Situ Formation of (PNP)Rh(H)(OTs)COPh (8), (PNP)RhOTs (9), and Free Benzaldehyde.** In a dry nitrogen glovebox, complex **5** (15 mg, 0.025 mmol) was charged in an NMR tube and dissolved in toluene-*d*<sub>8</sub> (0.5 mL). The solution was cooled to -30 °C by placing the tube in the freezer. Next, 1,4-dioxane (1 equiv, 2.2 mg) and TsOH (1 equiv, 4.3 mg) were added to the NMR tube, and it was taken out of the glovebox and put in the pre-cooled NMR spectrometer at 275 K. Spectra were recorded at various temperatures; however, coherent spectral data could only be obtained at 290 K. Due to overlapping of the various products, only partial assignment could be achieved of complex **8** (aromatic region signals overlapping solvent and benzaldehyde): <sup>1</sup>H NMR (500 MHz, toluene-*d*<sub>8</sub>, δ): 8.22 (d, <sup>3</sup>J<sub>HH</sub> = 6.1 Hz, 2H, TsO(H2,6)), 8.11 (d, <sup>3</sup>J<sub>HH</sub> = 5.4 Hz, 2H, COPh(H2,6)), 7.73 (t, <sup>3</sup>J<sub>HH</sub> = 7.6 Hz, 1H, Py-H4), 7.66 (d, <sup>3</sup>J<sub>HH</sub> = 7.6 Hz, 2H, Py-H3,5), 4.51, 3.59 (ABq, J<sub>AB</sub> = 17.0 Hz, 4H, CH<sub>2</sub>P) 2.14 (s, <sup>1</sup>H, OTs(CH<sub>3</sub>)), 1.18 (bvt, J<sub>PH</sub> = 6.7, 6.8 Hz, 18H, PC(CH<sub>3</sub>)<sub>3</sub>), 1.06 (bvt, J<sub>PH</sub> = 6.3, 6.4 Hz, 18H, PC(CH<sub>3</sub>)<sub>3</sub>), -19.13 (dt, <sup>1</sup>J<sub>RhH</sub> = 29.6 Hz, <sup>2</sup>J<sub>PH</sub> = 11.7 Hz, <sup>1</sup>H, Rh-H) ppm; <sup>13</sup>C{<sup>1</sup>H} NMR (125 MHz, toluene-*d*<sub>8</sub>, correlated by HSQC, δ): 37.1 (b, CH<sub>2</sub>P), 21.3 (OTs(CH<sub>3</sub>)), 29.5 (PC(CH<sub>3</sub>)<sub>3</sub>) ppm; <sup>31</sup>P{<sup>1</sup>H} NMR (202 MHz, toluene-*d*<sub>8</sub>, δ): 64.6 (bd, <sup>1</sup>J<sub>RhP</sub> = 114.61 Hz) ppm. At room temperature, within an hour, complexes **4c**, **9**, and **10** appear and are identifiable by <sup>31</sup>P{<sup>1</sup>H} NMR (202 MHz, toluene-*d*<sub>8</sub>, δ): 79.4 (d, <sup>1</sup>J<sub>RhP</sub> = 120.2 Hz, complex **4c**), 71.5 (d, <sup>1</sup>J<sub>RhP</sub> = 125.3 Hz, complex **10**), 60.3 (d, <sup>1</sup>J<sub>RhP</sub> = 147.3 Hz, complex **9**) ppm. Two other species form, which could not be unequivocally identified, and may be isomers of the identified complexes: <sup>31</sup>P{<sup>1</sup>H} NMR (202 MHz, toluene-*d*<sub>8</sub>, δ): 63.4 (d, <sup>1</sup>J<sub>RhP</sub> = 116.6 Hz, unknown), and 62.5 (d, <sup>1</sup>J<sub>RhP</sub> = 145.4 Hz, unknown) ppm. Brown crystals of complex **9**, suitable for X-ray crystallography, were collected from the toluene product mixture that was kept at -30 °C for a week. The crystal structure of complex **9** is depicted in Figure S54, and crystallographic data are given in Table S1 and the CIF file.

**Reaction of Complex 7 and TsOH: Formation of [(PNP)RhN<sub>2</sub>]TsO (10) and (PNP)RhOTs (9).** In a dry nitrogen glovebox, complex **7** (6.1 mg, 0.01 mmol) and TsOH (2.0 mg, 1 equiv) were dissolved in C<sub>6</sub>D<sub>6</sub> (0.5 mL). NMR spectroscopy revealed the formation of complexes **9** and **10** in a 1:9 ratio. Complex **10** is similar to previously reported [(PNP)RhN<sub>2</sub>]<sup>+</sup> fragments,<sup>59</sup> and was characterized by <sup>1</sup>H and <sup>31</sup>P NMR spectroscopy. The solution was then heated to 65 °C for 1 h, and complex **9** was formed in a 13:1 ratio to complex **10**. Complex **9**: <sup>1</sup>H NMR (400 MHz, benzene-*d*<sub>6</sub>, δ): 8.10 (d, <sup>3</sup>J<sub>HH</sub> = 8.1 Hz, 2H, OTs(H2,5)), 6.91 (d, <sup>3</sup>J<sub>HH</sub> = 7.9 Hz, 2H, OTs(H3,5)), 6.86 (t, <sup>3</sup>J<sub>HH</sub> = 7.6 Hz, 1H, Py-H4), 6.26 (d, <sup>3</sup>J<sub>HH</sub> = 7.6 Hz, 2H, Py-H2,3), 2.54 (vt, J<sub>PH</sub> = 3.3 Hz, 4H, CH<sub>2</sub>P), 2.00 (s, 3H, OTs(CH<sub>3</sub>)), 1.47–1.38 (bvt, J<sub>PH</sub> = 6.5, 6.6 Hz, 36H, PC(CH<sub>3</sub>)<sub>3</sub>) ppm; <sup>13</sup>C{<sup>1</sup>H} NMR (101 MHz, benzene-*d*<sub>6</sub>, δ): 165.90 (vt, J<sub>PC</sub> = 5.7 Hz, Py-C2,6), 144.53 (TsO-C4(ipso)), 138.67 (TsO-C1(C<sub>ipso</sub>SO)), 130.63 (Py-C4), 128.47 (OTs-C3,5), 127.13 (OTs-C2,6), 119.60 (vt, J<sub>PC</sub> = 4.7 Hz, Py-C3,5), 36.13 (vt, J<sub>PC</sub> = 5.6 Hz, CH<sub>2</sub>P), 34.49 (vt, J<sub>PC</sub> = 5.9, 6.5, PC(CH<sub>3</sub>)<sub>3</sub>), 29.38 (vt, J<sub>PC</sub> = 3.5 Hz, PC(CH<sub>3</sub>)<sub>3</sub>), 21.16 (OTs-CH<sub>3</sub>) ppm; <sup>31</sup>P{<sup>1</sup>H} NMR (162 MHz, benzene-*d*<sub>6</sub>, δ): 60.17 (d, <sup>1</sup>J<sub>RhP</sub> = 147.6 Hz) ppm. Complex **10**: <sup>1</sup>H NMR (300 MHz, benzene-*d*<sub>6</sub>, δ): 8.43 (overlapping doublets, <sup>3</sup>J<sub>HH</sub> = 6.0, 6.4 Hz, 4H, TsO<sup>-</sup>), 7.42 (t, <sup>3</sup>J<sub>HH</sub> = 7.8 Hz, 1H, Py-H4), 7.05 (d, <sup>3</sup>J<sub>HH</sub> = 7.9 Hz, 2H, Py-H3,5), 4.06 (vt, J<sub>PH</sub> = 3.9 Hz, 4H, CH<sub>2</sub>P), 2.10 (s, 3H, <sup>-</sup>OTs(CH<sub>3</sub>)), 1.19 (bvt, J<sub>PH</sub> = 13.9, 6.8 Hz, 36H, PC(CH<sub>3</sub>)<sub>3</sub>) ppm; <sup>31</sup>P{<sup>1</sup>H} NMR (121 MHz, benzene-*d*<sub>6</sub>, δ): 71.72 (d, <sup>1</sup>J<sub>RhP</sub> = 124.8 Hz). Another unidentified complex was formed with <sup>31</sup>P{<sup>1</sup>H} NMR (121 MHz, benzene-*d*<sub>6</sub>, δ): 62.5 (d, <sup>1</sup>J<sub>RhP</sub> = 145.5 Hz) ppm. This is possibly an isomer of complex

9, and appears in the reactions of TsOH with complex 5 (vide supra) but this could not be asserted, as its spectral features overlap with those of complex 9.

**Reaction of Complex 3 with TsOH: Independent Synthesis of [(PNP)RhCO]TsO (4c).** In a dry nitrogen glovebox, complex 3 (6.5 mg, 0.012 mmol) and TsOH (2.2 mg, 1.05 equiv) were mixed in C<sub>6</sub>D<sub>6</sub> (0.5 mL) in an NMR tube. The mixture was shaken vigorously for 15 min until the solution color turned from red to yellow, with the formation of the cationic complex 4c. The carbonyl IR stretch is at lower frequency than the previously reported [(PNP)RhCO]X (X = BF<sub>4</sub>, BAr<sup>f</sup>, OC(O)CF<sub>3</sub>, Cl),<sup>52</sup> suggesting partial coordination of the TsO<sup>-</sup> moiety. Reasonable solubility of the complex in benzene would suggest this as well. <sup>1</sup>H NMR (300 MHz, benzene-*d*<sub>6</sub>, δ): 8.53 (bd, <sup>3</sup>J<sub>HH</sub> = 7.0 Hz, 2H, Py-H3,5), 8.39 (d, <sup>3</sup>J<sub>HH</sub> = 7.9 Hz, 2H, TsO<sup>-</sup>(H2,6)), 7.60 (t, <sup>3</sup>J<sub>HH</sub> = 7.0 Hz, 1H, Py-H4), 7.04 (d, <sup>3</sup>J<sub>HH</sub> = 7.9 Hz, 2H TsO<sup>-</sup>(H3,5)), 4.24 (bvt, J<sub>PH</sub> = 3.6, 3.7 Hz 4H, CH<sub>2</sub>P), 2.10 (s, 3H, OTs(CH<sub>3</sub>)), 1.15 (bvt, J<sub>PH</sub> = 15.6, 8.4 Hz, 36H, PC(CH<sub>3</sub>)<sub>3</sub>) ppm; <sup>13</sup>C{<sup>1</sup>H} NMR (125 MHz, benzene-*d*<sub>6</sub>, δ): 196.24 (b, Rh-CO), 165.76 (vt, J<sub>PC</sub> = 5.7 Hz, Py-C2,6), 147.25 (TsO-C4(ipso)), 141.05 (Py-C4), 138.02 (TsO-C1(C<sub>ipso</sub>SO)), 128.57 (TsO<sup>-</sup>(C3,5)), 127.18 (TsO<sup>-</sup>(C3,5C2,6)), 123.72 (vt, J<sub>PC</sub> = 4.7 Hz, Py-C3,5), 36.25 (vt, J<sub>PC</sub> = 9.6 Hz, CH<sub>2</sub>P), 35.71 (vt, J<sub>PC</sub> = 9.2, PC(CH<sub>3</sub>)<sub>3</sub>), 29.24 (vt, J<sub>PC</sub> = 2.8 Hz, PC(CH<sub>3</sub>)<sub>3</sub>), 21.23 (OTs-CH<sub>3</sub>) ppm; <sup>31</sup>P{<sup>1</sup>H} NMR (121 MHz, benzene-*d*<sub>6</sub>, δ): 79.62 (d, <sup>1</sup>J<sub>RhP</sub> = 120.0 Hz). IR: ν<sub>CO</sub> = 1971 cm<sup>-1</sup>.

#### Sequential Photocarbonylation Cycles of Benzene with CO<sub>2</sub>.

**Caution!** H<sub>2</sub> gas is highly explosive, and appropriate safety measures should be taken when attempting these procedures. In a dry nitrogen glovebox, complex 1 (20.0 mg, 0.04 mmol) was dissolved in THF (0.5 mL) inside a J. Young NMR tube. The solution was frozen in liquid nitrogen and vacuum was pumped for 1 min, then let thaw, and opened to a 1 bar CO<sub>2</sub> atmosphere, sealed and shaken vigorously for 5 min. NMR spectroscopy showed formation of complex 2. The solution was shaken in the closed tube for 5 h, until NMR spectroscopy showed over 90% conversion to complex 3. The solution was then evaporated under high vacuum to dryness, and re-dissolved in benzene (1.5 mL) to fill the entire NMR tube volume. The benzene filled tube was introduced to the irradiation chamber and irradiated under UV(B) for 72 h. NMR spectroscopy showed formation of complexes 5 and 6 in a 5:1 ratio, respectively, with less than 5% unreacted complex 3. The solution was then transferred into a Schlenk flask in the dry nitrogen glovebox. TsOH (7.0 mg, 1 equiv to complex 1) was added and the solution was stirred for 24 h, during which the color changed from brown to yellow to dark red. The Schlenk flask was then connected to a receiver flask, and using freeze-pump technique all volatiles were distilled out and collected in the receiver flask. To the distillate solution was added mesitylene (5.6 mg, 0.046 mmol) as an internal standard and the amount of benzaldehyde thus produced was measured by <sup>1</sup>H NMR (7.2 × 10<sup>-3</sup> mmol, 18% overall yield relative to complex 1). In a dry nitrogen glovebox, to the dry organometallic residues from the reaction flask was added THF (1.5 mL) and potassium *tert*-butoxide (4.8 mg, 0.04 mmol). The solution was stirred for 3 h, and then evaporated under high vacuum. The solids were extracted to pentane (2 mL), filtered through Celite, and evaporated to dryness (20.2 mg of red solid obtained). NMR spectroscopy of the product showed formation of complexes 7 and 3 in a 3:1 ratio. This mixture was dissolved in pentane in a Fischer-Porter pressure vessel, pressed with 5.5 bar H<sub>2</sub> gas, and stirred for 2 days at room temperature. After evaporation of the volatiles, 18.9 mg of brown powder was obtained of complex 1 in a 3:1 mixture with complex 3 (93% Rh recovery). This mixture was dissolved in THF (0.5 mL) in a J. young NMR tube and the whole procedure was repeated as described above, producing additional 4.7 × 10<sup>-3</sup> mmol benzaldehyde (12% additional yield, relative to original amount of complex 1). Overall yield of benzaldehyde in two cycles (based on starting amount of complex 1) is 30%.

## ■ ASSOCIATED CONTENT

### Supporting Information

The Supporting Information is available free of charge on the ACS Publications website at DOI: 10.1021/jacs.6b05128.

NMR spectra for new complexes, additional experimental details, and spectral data, including Figures S1–S57, Scheme S1, and Table S1 (PDF)

X-ray crystallographic data for complexes 2, 3, 5, and 9 (CIF)

## ■ AUTHOR INFORMATION

### Corresponding Author

\*david.milstein@weizmann.ac.il

### Notes

The authors declare no competing financial interest.

## ■ ACKNOWLEDGMENTS

This research was supported by the Israel Science Foundation, and by the ASER (Alternative Sustainable Energy Research) fund. D.M. holds the Israel Matz Professorial Chair of Organic Chemistry.

## ■ REFERENCES

- (1) (a) Harlow, R. L.; Kinney, J. B.; Herskovitz, T. *J. Chem. Soc., Chem. Commun.* **1980**, 813–814. (b) Tominaga, K.-I.; Sasaki, Y. *Catal. Commun.* **2000**, 1, 1–3. (c) Tominaga, K.-I.; Sasaki, Y. *J. Mol. Catal. A: Chem.* **2004**, 220, 159–165.
- (2) (a) Fischer, R.; Langer, J.; Malassa, A.; Walther, D.; Görls, H.; Vaughan, G. *Chem. Commun.* **2006**, 2510–2512. (b) Silvia, J. S.; Cummins, C. C. *J. Am. Chem. Soc.* **2010**, 132, 2169–2171. (c) Mizuno, H.; Takaya, J.; Iwasawa, N. *J. Am. Chem. Soc.* **2011**, 133, 1251–1253. (d) Uhe, A.; Hölscher, M.; Leitner, W. *Chem. - Eur. J.* **2012**, 18, 170–177.
- (3) Ostapowicz, T. G.; Schmitz, M.; Krystof, M.; Klankermayer, J.; Leitner, W. *Angew. Chem., Int. Ed.* **2013**, 52, 12119–12123.
- (4) Liu, Q.; Wu, L.; Fleischer, I.; Selent, D.; Franke, R.; Jackstell, R.; Beller, M. *Chem. - Eur. J.* **2014**, 20, 6888–6894.
- (5) (a) Tani, Y.; Kuga, K.; Fujihara, T.; Terao, J.; Tsuji, Y. *Chem. Commun.* **2015**, 51, 13020–13023. (b) Xin, Z.; Lescot, C.; Friis, S. D.; Daasbjerg, K.; Skrydstrup, T. *Angew. Chem., Int. Ed.* **2015**, 54, 6862–6866. (c) Stieber, S. C. E.; Huguet, N.; Kageyama, T.; Jevtovikj, I.; Ariyananda, P.; Gordillo, A.; Schunk, S. A.; Rominger, F.; Hofmann, P.; Limbach, M. *Chem. Commun.* **2015**, 51, 10907–10909. (d) Masuda, Y.; Ishida, N.; Murakami, M. *J. Am. Chem. Soc.* **2015**, 137, 14063–14066. (e) Keane, A. J.; Farrell, W. S.; Yonke, B. L.; Zavalij, P. Y.; Sita, L. R. *Angew. Chem., Int. Ed.* **2015**, 54, 10220–10224. (f) Zhang, Z.; Liao, L.-L.; Yan, S.-S.; Wang, L.; He, Y.-Q.; Ye, J.-H.; Li, J.; Zhi, Y.-G.; Yu, D.-G. *Angew. Chem., Int. Ed.* **2016**, 55, 7068–7072.
- (6) Reviews: (a) Behr, A. *Chem. Ing. Tech.* **1985**, 57, 893–903. (b) Walther, D. *Coord. Chem. Rev.* **1987**, 79, 135–174. (c) Leitner, W. *Angew. Chem., Int. Ed. Engl.* **1995**, 34, 2207–2221. (d) Cokoja, M.; Bruckmeier, C.; Rieger, B.; Herrmann, W. A.; Kühn, F. E. *Angew. Chem., Int. Ed.* **2011**, 50, 8510–8537. (e) Huang, K.; Sun, C.-L.; Shi, Z.-J. *Chem. Soc. Rev.* **2011**, 40, 2435–2452. (f) Wu, L.; Liu, Q.; Jackstell, R.; Beller, M. *Angew. Chem., Int. Ed.* **2014**, 53, 6310–6320. (g) Liu, Q.; Wu, L.; Jackstell, R.; Beller, M. *Nat. Commun.* **2015**, 6, 5933.
- (7) Arakawa, H.; Aresta, M.; Armor, J. N.; Barteau, M. A.; Beckman, E. J.; Bell, A. T.; Bercaw, J. E.; Creutz, C.; Dinjus, E.; Dixon, D. A.; Domen, K.; DuBois, D. L.; Eckert, J.; Fujita, E.; Gibson, D. H.; Goddard, W. A.; Goodman, D. W.; Keller, J.; Kubas, G. J.; Kung, H. H.; Lyons, J. E.; Manzer, L. E.; Marks, T. J.; Morokuma, K.; Nicholas, K. M.; Periana, R.; Que, L.; Rostrup-Nielsen, J.; Sachtler, W. M. H.; Schmidt, L. D.; Sen, A.; Somorjai, G. A.; Stair, P. C.; Stults, B. R.; Tumas, W. *Chem. Rev.* **2001**, 101, 953–996.



- (8) Hossain, S. F.; Nicholas, K. M.; Teas, C. L.; Davis, R. E. *J. Chem. Soc., Chem. Commun.* **1981**, 268–269.
- (9) Lin, W.; Han, H.; Frei, H. *J. Phys. Chem. B* **2004**, *108*, 18269–18273.
- (10) Goettmann, F.; Thomas, A.; Antonietti, M. *Angew. Chem., Int. Ed.* **2007**, *46*, 2717–2720.
- (11) Gu, L.; Zhang, Y. *J. Am. Chem. Soc.* **2010**, *132*, 914–915.
- (12) Ménard, G.; Stephan, D. W. *Angew. Chem., Int. Ed.* **2011**, *50*, 8396–8399.
- (13) Palit, C. M.; Graham, D. J.; Chen, C.-H.; Foxman, B. M.; Ozerov, O. V. *Chem. Commun.* **2014**, *50*, 12840–12842.
- (14) Das Neves Gomes, C.; Blondiaux, E.; Thuéry, P.; Cantat, T. *Chem. - Eur. J.* **2014**, *20*, 7098–7106.
- (15) Zhang, M.; El-Roz, M.; Frei, H.; Mendoza-Cortes, J. L.; Head-Gordon, M.; Lacy, D. C.; Peters, J. C. *J. Phys. Chem. C* **2015**, *119*, 4645–4654.
- (16) Allen, O. R.; Dalgarno, S. J.; Field, L. D. *Organometallics* **2008**, *27*, 3328–3330.
- (17) Sampson, M. D.; Kubiak, C. P. *J. Am. Chem. Soc.* **2016**, *138*, 1386–1393.
- (18) Reviews: (a) Centi, G.; Perathoner, S. *Catal. Today* **2009**, *148*, 191–205. (b) Wang, W.; Wang, S.; Ma, X.; Gong, J. *Chem. Soc. Rev.* **2011**, *40*, 3703–3727.
- (19) Scheuermann, M. L.; Semproni, S. P.; Pappas, I.; Chirik, P. J. *Inorg. Chem.* **2014**, *53*, 9463–9465.
- (20) Riplinger, C.; Sampson, M. D.; Ritzmann, A. M.; Kubiak, C. P.; Carter, E. A. *J. Am. Chem. Soc.* **2014**, *136*, 16285–16298.
- (21) Reviews: (a) Tanaka, K. *Bull. Chem. Soc. Jpn.* **1998**, *71*, 17–29. (b) Jessop, P. G.; Ikariya, T.; Noyori, R. *Chem. Rev.* **1995**, *95*, 259–272. (c) Fukuzumi, S. *Eur. J. Inorg. Chem.* **2008**, *2008*, 1351–1362. (d) Alberico, E.; Nielsen, M. *Chem. Commun.* **2015**, *51*, 6714–6725. (e) Bo, C.; Dedieu, A. *Inorg. Chem.* **1989**, *28*, 304–309. (f) Hou, C.; Jiang, J.; Zhang, S.; Wang, G.; Zhang, Z.; Ke, Z.; Zhao, C. *ACS Catal.* **2014**, *4*, 2990–2997. (g) Mondal, B.; Neese, F.; Ye, S. *Inorg. Chem.* **2015**, *54*, 7192–7198. (h) Ni, S.-F.; Dang, L. *Phys. Chem. Chem. Phys.* **2016**, *18*, 4860–4870.
- (22) (a) Jessop, P. G.; Joó, F.; Tai, C. *Coord. Chem. Rev.* **2004**, *248*, 2425–2442. (b) Creutz, C.; Chou, M. H. *J. Am. Chem. Soc.* **2007**, *129*, 10108–10109. (c) Schmeier, T. J.; Hazari, N.; Incarvito, C. D.; Raskatov, J. A. *Chem. Commun.* **2011**, *47*, 1824–1826. (d) Schmeier, T. J.; Dobereiner, G. E.; Crabtree, R. H.; Hazari, N. *J. Am. Chem. Soc.* **2011**, *133*, 9274–9277.
- (23) (a) Tsai, J. C.; Nicholas, K. M. *J. Am. Chem. Soc.* **1992**, *114*, 5117–5124. (b) Graf, E.; Leitner, W. *J. Chem. Soc., Chem. Commun.* **1992**, 623–624. (c) Leitner, W.; Dinjus, E.; Gaßner, F. *J. Organomet. Chem.* **1994**, *475*, 257–266.
- (24) (a) Jessop, P. G.; Ikariya, T.; Noyori, R. *Nature* **1994**, *368*, 231–233. (b) Fornika, R.; Görls, H.; Seemann, B.; Leitner, W. *J. Chem. Soc., Chem. Commun.* **1995**, 1479–1481. (c) Jessop, P. G.; Hsiao, Y.; Ikariya, T.; Noyori, R. *J. Am. Chem. Soc.* **1996**, *118*, 344–355. (d) Joó, F.; Laurenczy, G.; Nádásdi, L.; Elek, J. *Chem. Commun.* **1999**, 971–972. (e) Tai, C.-C.; Pitts, J.; Linehan, J. C.; Main, A. D.; Munshi, P.; Jessop, P. G. *Inorg. Chem.* **2002**, *41*, 1606–1614. (f) Munshi, P.; Main, A. D.; Linehan, J. C.; Tai, C.-C.; Jessop, P. G. *J. Am. Chem. Soc.* **2002**, *124*, 7963–7971. (g) Ng, S. M.; Yin, C.; Yeung, C. H.; Chan, T. C.; Lau, C. P. *Eur. J. Inorg. Chem.* **2004**, *2004*, 1788–1793. (h) Hayashi, H.; Ogo, S.; Fukuzumi, S. *Chem. Commun.* **2004**, 2714–2715.
- (25) (a) Tanaka, R.; Yamashita, M.; Nozaki, K. *J. Am. Chem. Soc.* **2009**, *131*, 14168–14169. (b) Federsel, C.; Boddien, A.; Jackstell, R.; Jennerjahn, R.; Dyson, P. J.; Scopelliti, R.; Laurenczy, G.; Beller, M. *Angew. Chem., Int. Ed.* **2010**, *49*, 9777–9780. (c) Hull, J. F.; Himeda, Y.; Wang, W.-H.; Hashiguchi, B.; Periana, R.; Szalda, D. J.; Muckerman, J. T.; Fujita, E. *Nat. Chem.* **2012**, *4*, 383–388.
- (26) Langer, R.; Diskin-Posner, Y.; Leitus, G.; Shimon, L. J. W.; Ben-David, Y.; Milstein, D. *Angew. Chem., Int. Ed.* **2011**, *50*, 9948–9952.
- (27) Kang, P.; Cheng, C.; Chen, Z.; Schauer, C. K.; Meyer, T. J.; Brookhart, M. *J. Am. Chem. Soc.* **2012**, *134*, 5500–5503.
- (28) (a) Filonenko, G. A.; Conley, M. P.; Copéret, C.; Lutz, M.; Hensen, E. J. M.; Pidko, E. A. *ACS Catal.* **2013**, *3*, 2522–2526.
- (b) Moret, S.; Dyson, P. J.; Laurenczy, G. *Nat. Commun.* **2014**, *5*, 4017. (c) Nakada, A.; Koike, K.; Nakashima, T.; Morimoto, T.; Ishitani, O. *Inorg. Chem.* **2015**, *54*, 1800–1807. (d) Watari, R.; Kayaki, Y.; Hirano, S.-I.; Matsumoto, N.; Ikariya, T. *Adv. Synth. Catal.* **2015**, *357*, 1369–1373. (e) Chakraborty, S.; Blacque, O.; Berke, H. *Dalton Trans.* **2015**, *44*, 6560–6570.
- (29) Lilio, A. M.; Reineke, M. H.; Moore, C. E.; Rheingold, A. L.; Takase, M. K.; Kubiak, C. P. *J. Am. Chem. Soc.* **2015**, *137*, 8251–8260.
- (30) Zhang, Y.; Williard, P. G.; Bernskoetter, W. H. *Organometallics* **2016**, *35*, 860–865.
- (31) Reviews: (a) Wang, W.-H.; Himeda, Y.; Muckerman, J. T.; Manbeck, G. F.; Fujita, E. *Chem. Rev.* **2015**, *115*, 12936–12973. (b) Mellmann, D.; Sponholz, P.; Junge, H.; Beller, M. *Chem. Soc. Rev.* **2016**, *45*, 3954–3988.
- (32) Zell, T.; Butschke, B.; Ben-David, Y.; Milstein, D. *Chem. - Eur. J.* **2013**, *19*, 8068–8072.
- (33) Jongbloed, L. S.; de Bruin, B.; Reek, J. N. H.; Lutz, M.; van der Vlugt, J. I. *Catal. Sci. Technol.* **2016**, *6*, 1320–1327.
- (34) Federsel, C.; Jackstell, R.; Beller, M. *Angew. Chem., Int. Ed.* **2010**, *49*, 6254–6257.
- (35) (a) Rezaee, N. M.; Huff, C. A.; Sanford, M. S. *J. Am. Chem. Soc.* **2015**, *137*, 1028–1031. (b) Khusnutdinova, J. R.; Garg, J. A.; Milstein, D. *ACS Catal.* **2015**, *5*, 2416–2422. (c) Kothandaraman, J.; Goepfert, A.; Czaun, M.; Olah, G. A.; Prakash, G. K. S. *J. Am. Chem. Soc.* **2016**, *138*, 778–781.
- (36) (a) Zhang, L.; Han, Z.; Zhao, X.; Wang, Z.; Ding, K. *Angew. Chem., Int. Ed.* **2015**, *54*, 6186–6189. (b) Kang, B.; Hong, S. H. *Adv. Synth. Catal.* **2015**, *357*, 834–840.
- (37) (a) Hutschka, F.; Dedieu, A.; Leitner, W. *Angew. Chem., Int. Ed. Engl.* **1995**, *34*, 1742–1745. (b) Huang, K.-W.; Han, J. H.; Musgrave, C. B.; Fujita, E. *Organometallics* **2007**, *26*, 508–513. (c) Vignalok, A.; Ben-David, Y.; Milstein, D. *Organometallics* **1996**, *15*, 1839–1844. (d) Musashi, Y.; Sakaki, S. *J. Chem. Soc., Dalton Trans.* **1998**, 577–584. (e) Pomelli, C. S.; Tomasi, J.; Solá, M. *Organometallics* **1998**, *17*, 3164–3168. (f) Yoshida, T.; Thorn, D. L.; Okano, T.; Ibers, J. A.; Otsuka, S. *J. Am. Chem. Soc.* **1979**, *101*, 4212–4221.
- (38) Musashi, Y.; Sakaki, S. *J. Am. Chem. Soc.* **2002**, *124*, 7588–7603.
- (39) Reviews: (a) Khusnutdinova, J. R.; Milstein, D. *Angew. Chem., Int. Ed.* **2015**, *54*, 12236–12273. (b) Gunanathan, C.; Milstein, D. In *Bond Activation by Metal-Ligand Cooperation: Design of “Green” Catalytic Reactions Based on Aromatization–Dearomatization of Pincer Complexes*; Ikariya, T., Shibasaki, M., Eds.; Springer: Berlin/Heidelberg, 2011; Vol. 37, pp 55–84. (c) Zell, T.; Milstein, D. *Acc. Chem. Res.* **2015**, *48*, 1979–1994. (d) Gunanathan, C.; Milstein, D. *Acc. Chem. Res.* **2011**, *44*, 588–602.
- (40) (a) Montag, M.; Zhang, J.; Milstein, D. *J. Am. Chem. Soc.* **2012**, *134*, 10325–10328. (b) Zhang, J.; Leitner, G.; Ben-David, Y.; Milstein, D. *J. Am. Chem. Soc.* **2005**, *127*, 10840–10841. (c) Gunanathan, C.; Ben-David, Y.; Milstein, D. *Science* **2007**, *317*, 790–792. (d) Fogler, E.; Garg, J. A.; Hu, P.; Leitner, G.; Shimon, L. J. W.; Milstein, D. *Chem. - Eur. J.* **2014**, *20*, 15727–15731. (e) Hu, P.; Diskin-Posner, Y.; Ben-David, Y.; Milstein, D. *ACS Catal.* **2014**, *4*, 2649–2652.
- (41) (a) Gunanathan, C.; Gnanaprakasam, B.; Iron, M. A.; Shimon, L. J. W.; Milstein, D. *J. Am. Chem. Soc.* **2010**, *132*, 14763–14765. (b) Balaraman, E.; Gnanaprakasam, B.; Shimon, L. J. W.; Milstein, D. *J. Am. Chem. Soc.* **2010**, *132*, 16756–16758. (c) Feller, M.; Diskin-Posner, Y.; Shimon, L. J. W.; Ben-Ari, E.; Milstein, D. *Organometallics* **2012**, *31*, 4083–4101.
- (42) (a) Vogt, M.; Nerush, A.; Iron, M. A.; Leitner, G.; Diskin-Posner, Y.; Shimon, L. J. W.; Ben-David, Y.; Milstein, D. *J. Am. Chem. Soc.* **2013**, *135*, 17004–17018. (b) Nerush, A.; Vogt, M.; Gellrich, U.; Leitner, G.; Ben-David, Y.; Milstein, D. *J. Am. Chem. Soc.* **2016**, *138*, 6985–6997.
- (43) Anaby, A.; Butschke, B.; Ben-David, Y.; Shimon, L. J. W.; Leitner, G.; Feller, M.; Milstein, D. *Organometallics* **2014**, *33*, 3716–3726.
- (44) Zhang, J.; Leitner, G.; Ben-David, Y.; Milstein, D. *Angew. Chem., Int. Ed.* **2006**, *45*, 1113–1115.
- (45) Schwartsburd, L.; Iron, M. A.; Konstantinovski, L.; Ben-Ari, E.; Milstein, D. *Organometallics* **2011**, *30*, 2721–2729.

(47) Langer, R.; Leitus, G.; Ben-David, Y.; Milstein, D. *Angew. Chem., Int. Ed.* **2011**, *50*, 2120–2124.

(48) Feller, M.; Ben-Ari, E.; Diskin-Posner, Y.; Carmieli, R.; Weiner, L.; Milstein, D. *J. Am. Chem. Soc.* **2015**, *137*, 4634–4637.

(49) Gunanathan, C.; Milstein, D. *Science* **2013**, *341*, 1229712.

(50) (a) Vogt, M.; Rivada-Wheelaghan, O.; Iron, M. A.; Leitus, G.; Diskin-Posner, Y.; Shimon, L. J. W.; Ben-David, Y.; Milstein, D. *Organometallics* **2013**, *32*, 300–308. (b) Vogt, M.; Gargir, M.; Iron, M. A.; Diskin-Posner, Y.; Ben-David, Y.; Milstein, D. *Chem. - Eur. J.* **2012**, *18*, 9194–9197.

(51) Feller, M.; Gellrich, U.; Anaby, A.; Diskin-Posner, Y.; Milstein, D. *J. Am. Chem. Soc.* **2016**, *138*, 6445–6454.

(52) Feller, M.; Ben-Ari, E.; Gupta, T.; Shimon, L. J. W.; Leitus, G.; Diskin-Posner, Y.; Weiner, L.; Milstein, D. *Inorg. Chem.* **2007**, *46*, 10479–10490.

(53) Feller, M.; Ben-Ari, E.; Iron, M. A.; Diskin-Posner, Y.; Leitus, G.; Shimon, L. J. W.; Konstantinovski, L.; Milstein, D. *Inorg. Chem.* **2010**, *49*, 1615–1625.

(54) Iron, M. A.; Ben-Ari, E.; Cohen, R.; Milstein, D. *Dalton Trans.* **2009**, 9433–9439.

(55) Bennett, M. A. *J. Mol. Catal.* **1987**, *41*, 1–20.

(56) (a) Sakaki, S.; Musashi, Y. *Int. J. Quantum Chem.* **1996**, *57*, 481–491. (b) Musashi, Y.; Sakaki, S. *J. Am. Chem. Soc.* **2000**, *122*, 3867–3877. (c) Ohnishi, Y.; Matsunaga, T.; Nakao, Y.; Sato, H.; Sakaki, S. *J. Am. Chem. Soc.* **2005**, *127*, 4021–4032. (d) Pu, L. S.; Yamamoto, A.; Ikeda, S. *J. Am. Chem. Soc.* **1968**, *90*, 3896–3896.

(57) Calabrese, J. C.; Herskovitz, T.; Kinney, J. B. *J. Am. Chem. Soc.* **1983**, *105*, 5914–5915.

(58) (a) Grushin, V. V.; Kuznetsov, V. F.; Bensimon, C.; Alper, H. *Organometallics* **1995**, *14*, 3927–3932. (b) Kaska, W. C.; Nemeš, S.; Shirazi, A.; Potuznik, S. *Organometallics* **1988**, *7*, 13–15.

(59) (a) Hanson, S. K.; Heinekey, D. M.; Goldberg, K. I. *Organometallics* **2008**, *27*, 1454–1463. (b) Kloek, S.; Heinekey, D. M.; Goldberg, K. I. *Angew. Chem., Int. Ed.* **2007**, *46*, 4736–4738.

(60) (a) Boese, W. T.; Goldman, A. S. *J. Am. Chem. Soc.* **1992**, *114*, 350–351. (b) Maguire, J. A.; Boese, W. T.; Goldman, M. E.; Goldman, A. S. *Coord. Chem. Rev.* **1990**, *97*, 179–192.

(61) Rosini, G. P.; Boese, W. T.; Goldman, A. S. *J. Am. Chem. Soc.* **1994**, *116*, 9498–9505.

(62) (a) Jones, W. D.; Feher, F. J. *J. Am. Chem. Soc.* **1984**, *106*, 1650–1663. (b) Ghosh, C. K.; Graham, W. A. G. *J. Am. Chem. Soc.* **1987**, *109*, 4726–4727. (c) Spillett, C.; Ford, P. C. *J. Am. Chem. Soc.* **1989**, *111*, 1932–1933.

(63) Boyd, S. E.; Field, L. D.; Partridge, M. G. *J. Am. Chem. Soc.* **1994**, *116*, 9492–9497.

(64) (a) Kunin, A. J.; Eisenberg, R. *Organometallics* **1988**, *7*, 2124–2129. (b) Kunin, A. J.; Eisenberg, R. *J. Am. Chem. Soc.* **1986**, *108*, 535–536. (c) Fisher, B. J.; Eisenberg, R. *Organometallics* **1983**, *2*, 764–767.

(65) Sakakura, T.; Tanaka, M. *Chem. Lett.* **1987**, *16*, 249–252.

(66) Kläui, W.; Schramm, D.; Peters, W. *Eur. J. Inorg. Chem.* **2001**, *2001*, 3113–3117.

(67) (a) Hasanayn, F.; Abu-El-Ez, D. *Inorg. Chem.* **2010**, *49*, 9162–9168. (b) Anderson, G. K.; Cross, R. J. *Acc. Chem. Res.* **1984**, *17*, 67–74. (c) Calderazzo, F. *Angew. Chem., Int. Ed. Engl.* **1977**, *16*, 299–311. (d) Kuhlmann, E. J.; Alexander, J. J. *Coord. Chem. Rev.* **1980**, *33*, 195–225.

(68) Water contamination or protic conditions cause protonation of complex **3** to the aromatic cationic form (complex **4a** in the case of water), evident as a doublet at 79.5 ppm ( $^1J_{\text{RHP}} = 120$  Hz) in the  $^{31}\text{P}\{^1\text{H}\}$  NMR spectrum, which does not react at all under UV irradiation.

(69) Classic synthesis of benzaldehyde: Gattermann, L.; Koch, J. A. *Ber. Dtsch. Chem. Ges.* **1897**, *30*, 1622–1624.

(70) Goikhman, R.; Milstein, D. *Angew. Chem., Int. Ed.* **2001**, *40*, 1119–1122.

(71) Although a catalytic reaction of benzene carbonylation to benzaldehyde is thermodynamically uphill, further hydrogenation of benzaldehyde to benzyl alcohol would result in a close to

thermoneutral process (Haynes, W. M., Ed. *CRC Handbook of Chemistry and Physics*, 96th ed.; CRC Press, Taylor and Francis Group, LLC: Boca Raton, FL, 2015), potentially leading to a catalytically viable process for reductive carbonylation of arenes.

(72) Fulmer, G. R.; Miller, A. J. M.; Sherden, N. H.; Gottlieb, H. E.; Nudelman, A.; Stoltz, B. M.; Bercaw, J. E.; Goldberg, K. I. *Organometallics* **2010**, *29*, 2176–2179.